ELSEVIER

Chemical Engineering Science 59 (2004) 2619–2632

Chemical Engineering Science

www.elsevier.com/locate/ces

Dynamic and steady-state sedimentation of polydisperse suspension and prediction of outlets particle-size distribution

A. Zeidan, S. Rohani*, A. Bassi

Department of Chemical and Biochemical Engineering, Faculty of Engineering Science, University of Western Ontario, London, Ont., Canada N6A 5B9

Received 26 November 2002; received in revised form 15 July 2003; accepted 7 January 2004

Available online 14 May 2004

Abstract

The Kynch theorem was extended to non-linear system of conservation laws of polydisperse suspensions of spherical particles. The simulation predicts overflow of light particles and heavy particles at steady state and dynamic mode of batch and continuous sedimentation. The model eliminated the need for imposed non-theoretical parameters or functions to predict hindered settling and effluent concentrations. Particle-size distribution is also predicted at the effluent and the underflow. We examined several cases and predicted dynamic behaviour of rarefaction waves and overloaded continuous settler. A new concept of dynamic flux curves is also used and introduced.

Keywords: Mathematical; Modeling; Sedimentation; Hydrodynamics; Settling velocity; Polydisperse

1. Introduction

Continuous sedimentation is a widely used process for solid–liquid separation. Continuous sedimentation takes place in a clarifier-thickener unit with one input stream at some point in the middle and two outputs at the top and the bottom of the unit. The simulation of the settler's concentration profiles at the outputs as well as the interior of the unit has always been a challenging mathematical problem. Several models have simulated the thickening section of the settler without considering the clarifier. Other models often used imposed parameters or feed-dependent functions to represent the light particles in the overflow. Some models successfully predicted effluent concentration using certain flux-based models but without predicting particle-size distribution. This paper will discuss these models and present a numerical simulation technique capable of predicting the behaviour of particles of different sizes and densities at the interior and the output streams of the settler.

* Corresponding author. Tel.: +1-519-661-2131; fax: +1-519-661-3498.
E-mail address: rohani@eng.uwo.ca (S. Rohani).

0009-2509/$ - see front matter © 2004 Published by Elsevier Ltd.
doi:10.1016/j.ces.2004.01.064

2. Theory

Discussion of the theory of sedimentation involves several topics that will be covered in the coming subsections. Topics discussed include settling velocity, flux curve, discontinuities, and numerical methods.

2.1. Settling velocity

Settling velocity of a particle is a basic constitutive phenomenon of the sedimentation process where particles settle due to gravity to the bottom of the settler. In a batch settler, particles with positive settling velocity would settle and particles with negative settling velocity rise to the top. In a continuous secondary settler, particles with settling velocity larger than the liquid effluent bulk velocity will settle. Other particles will leave with the overflow stream. Fig. 1 shows a systematic flow diagram of a continuous settler. Several settling velocity models exist in the literature based on analytical, empirical, semi-empirical, and flux-based solutions.

Flux-based empirical settling velocity models are developed specifically to determine a flux curve accurately close in shape to the typical flux curves obtained from sedimentation experiments. These models are limited in their

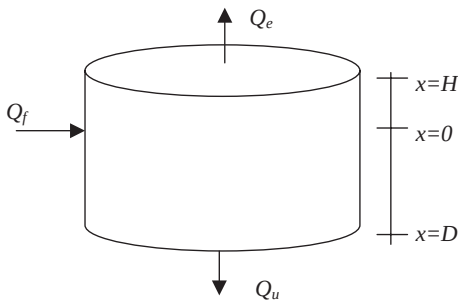

Fig. 1. Ideal settler with a constant area.

applicability because they include experimentally determined parameters. That is, they are limited to the suspensions investigated and might not be useful for a different suspension system. They are also independent of particle-size distribution and density distribution. Several researchers have developed such models like Vesilind (1979), Härtel and Pöpel (1992), Takacs et al. (1991), Cho et al. (1993), Font and Ruiz (1993) and Mazzolani et al. (1998). These models can be used efficiently for the simulation of the sedimentation of flocculated particles as shown in several papers by Takacs et al. (1991), Hamilton et al. (1992), Otterpohl and Freund (1992), Härtel and Pöpel (1992), Dupont and Henze (1992), Font and Ruiz (1993), Grijspeerdt et al. (1995), Zheng and Bagley (1998), Jeppsson and Diehl (1996), Diehl and Jeppsson (1998), Bürger and Concha (1998), Bürger et al. (1999), Bürger et al. (2000a,b), and Garrido et al. (2000). For most purposes, these models are sufficient. But when the prediction of the particle-size distribution is required or when the suspension quality of the modeled system is not constant, these settling velocity models are not widely applicable.

Settling velocity models that depend on particle size and density were investigated thoroughly and various equations were given (Zeidan et al., 2003a). The particle–liquid and particle–particle interaction models are usually useful for applications that require predicting the settling velocities in polydisperse suspension using particle size and density. These models vary in their validity and applicability. The basic Stokes equation is only valid for spheres in infinite fluid medium. Richardson and Zaki (1954) equation was developed on the basis of monodisperse suspension examined at different Reynolds number regions using several experimental data. Garside and Al-Dibouni (1977) noticed that settling velocity data take a "logistic" shape and developed their model based on this observation. Richardson and Zaki correlation and Garside and Al-Dibouni equations are known to give good prediction of the experimental data of monodisperse suspensions. They are also used widely in many papers for comparison purposes. Barnea and Mizrahi (1973), on the other hand, considered the hydrostatic effect, momentum transfer, wall effects, and analytical solution. The model parameters were also obtained based on several experimental data and it also gave good predictions for monodisperse suspensions. Lockett and Al-Habbooby (1973) suggested the use of total solid volume fraction instead of component solid volume fraction for multi-size suspensions, which is considered an extension of Richardson and Zaki and other models. Doheim et al. (1997) work is also an extension of Richardson and Zaki to obtain better predictions for multi-particle suspension. Dallavalle's model (1948) is based on an approximation of the drag factor and is suitable for all *Re* values and monodisperse suspensions. Quispe et al. (2000) introduced a model that involves a best-fit parameter.

Particle–particle interaction equations extend the validity of the above models to multi-particles systems of different sizes and densities. Examples of particle–particle interaction models are Mirza and Richardson (1978), Masliyah (1979), Patwardhan and Tien (1985), Zimmels (1983), Williams and Amarasinghe (1989), Selim et al. (1983), and Chueng et al. (1996) models. A complete discussion and comparison of a wide selection of the above models for the best fit with experimental data was presented by Zeidan et al. (2003a) and concluded that two models provide the best prediction, which are Richardson and Zaki correlation coupled with Masliyah model and Garside and Al-Dibouni correlation coupled with Selim, Kothari, and Turian model (Zeidan et al., 2003a).

2.2. Flux curves

The fluid bulk velocities of downward and upward flows are given by the following equations:

$$v_{f,u} = \frac{Q_u}{A},$$

$$v_{f,e} = \frac{Q_e}{A}, \tag{1}$$

where $v_{f,u}$ is the bulk velocity of the underflow, $v_{f,e}$ is the bulk velocity of the overflow, Q_u is the underflow flow rate, Q_e is the overflow flow rate and A is the cross-sectional area of the settler assumed to be constant. The batch flux $f_b(c)$ is given by the following equation:

$$f_b(c) = v_s c, \tag{2}$$

where c is the solids concentration and v_s is the particle settling velocity due to gravity. The downward flux curve $f(c)$ is described by the following equation:

$$f(c) = f_b(c) + v_{f,u} c \tag{3}$$

and the upward flux $g(c)$ is described as follows:

$$g(c) = f_b(c) - v_{f,e} c. \tag{4}$$

A typical flux curve for batch and continuous settling is shown in Fig. 2. At very high bulk velocities the flux curves $f(c)$ and $g(c)$ become straight lines.

It should be noted that assuming a constant cross-sectional area is valid since most secondary clarifiers have constant

cross-sectional area except the bottom, where continuous removal of the sludge is active. Our model is based on such criteria, but it should be noted that the simulation is extendable to settlers of varying cross-sectional areas, which is left for the future development and examination of the model.

2.3. Sedimentation model

One-dimensional models of the continuous settler are based on dividing the settlers into several layers, where the concentration of solids is determined only by the conservation of mass in 1D mathematical model. Two- and three-dimensional models exist in the literature, but their simulation is time consuming and difficult to verify experimentally Grijspeerdt et al. (1995).

Solving mass balance around each layer using a proper numerical method is the key for dynamic simulation of the thickener, which will be discussed later. A layer could be represented as a grid point on a one-dimensional domain representing the settler height. The feed input is modelled by a point source and the solids entering the settler are assumed to distribute instantly in the entire cross-section of the feed layer or grid. The regime above the feed point is called the *clarification zone* and the one below the feed point is described as the *thickening zone*. The settler is assumed to behave ideally without considering factors such as turbulence or density currents. The settling process is assumed to occur in the settler stages and not in the outlet streams. A basic assumption of the Kynch (1952) theorem on sedimentation is that the mass flux is only based on the local concentration.

2.4. Critical review

Kynch (1952) was the first to propose a kinematical model for sedimentation, which was based on the propagation of kinematic waves in a suspension. The batch sedimentation process is described by a continuity equation of the solid particles

$$\frac{\partial c(x)}{\partial t} + \frac{\partial f_b(c(x))}{\partial x} = 0, \tag{5}$$

where t is time, $c(x)$ is the solids concentration at settler height x and $f_b(c(x))$ is the batch flux function. Kynch showed that knowledge of the function $f_b(c(x))$ is enough to construct the method of characteristics using the following initial condition in a batch sedimentation:

$$c(x) = \left\{ \begin{array}{ll} 0 & x = L \\ c_0 & 0 < x < L \\ c_{\max} & x = 0 \end{array} \right\}, \tag{6}$$

where c_0 is the initial homogeneous suspension concentration, $c_{\max}$ is the maximum attainable concentration, and L is the depth of the batch sedimentation tank. Kynch showed that an extremely rapid increase of concentration from initial value to the maximum attainable value at the bottom of the settler occurs.

Petty (1975) was among the first to provide theoretical basis to extend Kynch batch settling analysis to continuous sedimentation. Several papers studied the continuous sedimentation with a feed and two outlets streams. The goal of settler modelling is to predict the outlets and the internal concentration profiles at any feed concentration condition at steady state or in a dynamic mode. Consequently, it is important to predict the sludge blanket discontinuity that appears in the settler under normal operating conditions.

Bustos et al. (1990) used Petty's work and investigated a simple model for continuous sedimentation. Shortcomings of the model include the inability to predict the *clarification zone* profile and the overflow concentration.

Härtel and Pöpel (1992) divided the settler into horizontal imaginary layers and estimated the underflow concentration by introducing a factor that depends on the height and the sludge volume index, SVI. It ensured simulating hindered settling at the feed and a thickening behaviour at the bottom. The use of Stokes' equation for effluent modelling limited the overflow simulation to dilute and small particles present in the *clarification zone*.

Otterpohl and Freund (1992) used Härtel and Pöpel's work and applied the minimal condition on the flux equation of the *thickening zone*, which limits the amount of sediment in each layer. Such condition is not based on mathematical and theoretical bases and is used to simulate hindered settling as observed in typical sedimentation processes.

One shortcoming of many sedimentation simulations is the inability to predict effluent concentrations because the settling velocity functions used usually predicts an average downward settling velocity. Dupont and Henze (1992) proposed an equation that can predict the amount of particulates in the overflow for a given feed input. On the other hand, Takacs et al. (1991) used a settling velocity function with two exponential terms: one represents the particles in the underflow and the other represents the particles in the overflow. The minimal condition was also used to restrict flux flow from an upper layer to a lower layer, but a threshold parameter was used in the clarification regime where if the concentration is less than the threshold value, the minimum condition is not applied. Watts et al. (1996), Hamilton et al. (1992), and Lev et al. (1986) replaced the minimal condition with a dispersion parameter.

The bottom of settler could involve compression of the sedimentation, which is generally modelled by a partial differential equation with a non-linear diffusion term. In the simulation presented in this document, compression effects were not considered. It should be noted that the compression phenomenon is considered different than the thickening phenomenon. The thickening results in a rapid increase of concentration at the bottom of the settler that would lead to a sludge blanket. Compression may then occur due to the increase of sludge weight. Concha and Bustos (1987), Font and Ruiz (1993), Zheng and Bagley (1998), Bürger

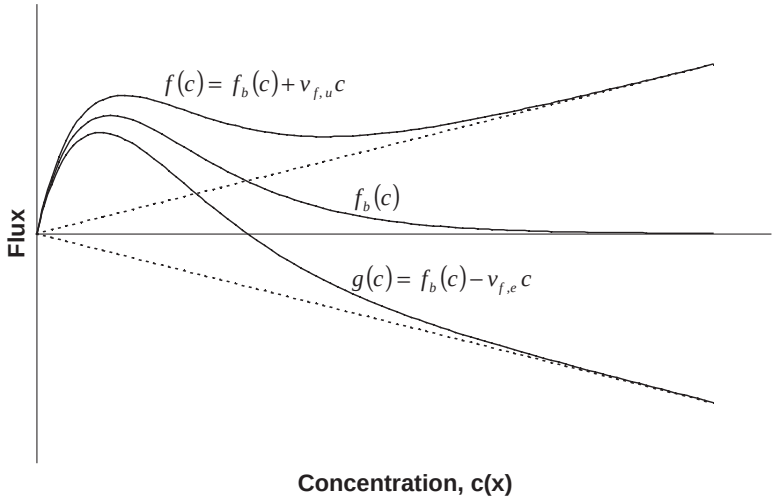

Fig. 2. The flux curves $f(c)$, $f_b(c)$ and $g(c)$. The top dashed straight line is the underflow operating line $cv_{f,u}$ and the bottom dashed straight line is the effluent operating line $cv_{f,e}$.

and Concha (1998), Bürger et al. (1999, 2000a,b, 2001), and Garrido et al. (2000) discussed modelling sedimentation with a compression zone.

In general, many of the previous models failed to predict effluent concentration or used imposed parameters. Other models were successful in predicting effluent concentrations, but failed to predict particle-size distribution explicitly because they used flux-based settling velocity models. On the other hand, a recent article by Bürger et al. (2000c) provided a modern dynamic simulation of multi-particle suspensions using a numerical scheme that they developed. In the work presented here, the same ideas were shared but using a different numerical simulation based on the Godunov numerical scheme and Diehl's (1996, 1997) work that describes discontinuities of the input and outputs. Godunov scheme is considered a powerful numerical method for discontinuous hyperbolic problems and the reason will be discussed later.

2.5. Model development and shocks

Our model is based on the dynamic and steady-state modelling of the whole settler discussed by Chancelier et al. (1994) and Diehl (1996, 1997). Under the prescribed assumption known as the ideal sedimentation, Diehl evaluated the settler behaviour based on a partial differential hyperbolic equation with a feed-point source term and discontinuous flux function using the Godunov numerical scheme.

An entropy condition introduced by Diehl (1995,1996, 1997) was used to solve the discontinuities at the top, feed, and the bottom. Thus, Diehl assumed that the boundary conditions at the feed inlet as well as the top and bottom outlets are part of the solution and cannot be prescribed. In other words, the only correct boundary condition at outlets is the one with a flux equal to the one inside the settler just before the outlets.

The continuous settler could be presented by a partial differential equation

$$\frac{\partial c(x)}{\partial t} + \frac{\partial f(c(x))}{\partial x} = s(t)\delta(x), \tag{7}$$

where $f(c(x))$ is the flux function, $s(t)$ is the source or feed function, and $\delta(x)$ is the delta function. The flux function is a discontinuous function described in the following relationship for a settler of a cylindrical shape with a constant cross-sectional area:

$$f(c(x)) = \begin{Bmatrix} -v_{f,e}c & x < -H \\ g(c) = f_b(c) - v_{f,e}c & -H < x < 0 \\ f(c) = f_b(c) + v_{f,u}c & 0 < x < D \\ v_{f,u}c & x > D \end{Bmatrix}, \tag{8}$$

where H is the clarifier section height and D is the thickening section depth. Fig. 2 shows a representation of such unit. Eq. (7) reduces to the following equation when examining a point above or below the feed point:

$$\frac{\partial c(x)}{\partial t} + \frac{\partial f(c(x))}{\partial x} = 0. \tag{9}$$

The solution of the equation could be constructed based on the method of characteristics but non-unique solution occurs because of the formation of discontinuities. Discontinuities are generated when the straight characteristic lines propagating at constant concentration with time intersect. This happens because of the non-linearity of the flux function, which causes concentration waves to propagate at different speeds and interact to form discontinuities.

Entropy conditions and viscous profiles are introduced to resolve the non-uniqueness of these discontinuities. The purpose is to reject unstable discontinuities and calculate

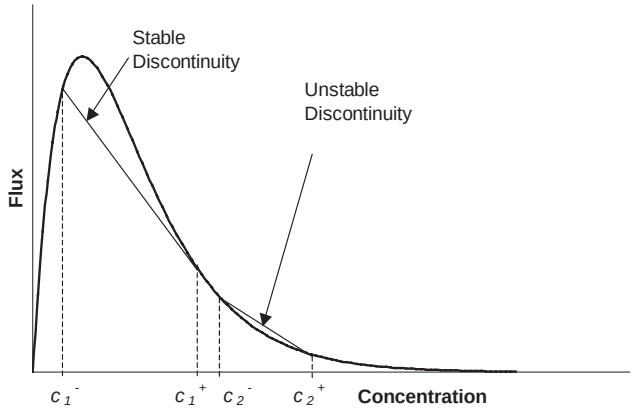

Fig. 3. Stable and unstable discontinuities in a batch flux curve.

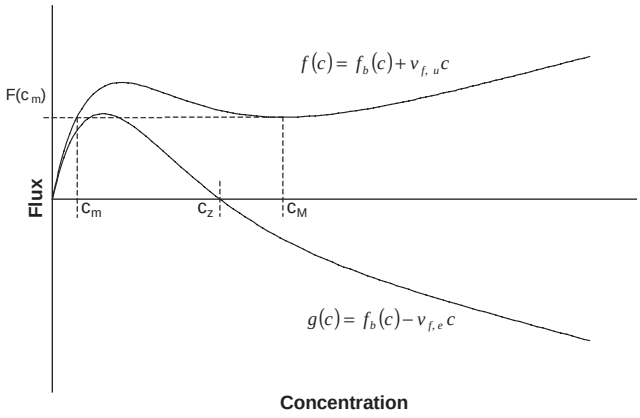

Fig. 4. Points c_m, c_M and c_z at flux curve.

the speed of stable discontinuities. For example, a unique physical solution could be obtained by adding a diffusion (viscous) term to Eq. (9) as follows:

$$\frac{\partial c(x)}{\partial t} + \frac{\partial f(c(x))}{\partial x} = \varepsilon \frac{\partial^2 c(x)}{\partial x}, \tag{10}$$

where ε is a small positive diffusivity parameter. Eq. (10) has a unique smooth solution for a given initial data. Letting $\varepsilon \to 0$ provides a limit solution with discontinuities for Eq. (7). Another approach is by acknowledging that a discontinuity should be stable under disturbances. If across a discontinuity a sudden appearance of concentration $c(x)$ at time t_1 occurs between the concentrations $c(x^-)$ and $c(x^+)$ at the sides of the discontinuity, then a stable discontinuity would reassert itself at time $t > t_1$. Lax (1957) and Lax and Wendroff (1960) have translated the above condition to a mathematical generalized entropy condition

$$\frac{f(c(x)) - f(c(x^-))}{c(x) - c(x^-)} \geqslant \frac{f(c(x^+)) - f(c(x^-))}{c(x^+) - c(x^-)}$$
$$x \in (x^-, x^+) \tag{11}$$

where $c(x^+)$ and $c(x^-)$ are the concentrations below and above the discontinuity, respectively. The equation must be valid for all $c(x)$ between $c(x^-)$ and $c(x^+)$ in order to have a stable discontinuity. The condition states that a stable discontinuity only exists when the graph of $f(c(x))$ lies above (below) the chord joining the points $c(x^-)$ and $c(x^+)$ when $c(x^-)$ is smaller (greater) than $c(x^+)$. The condition implies that characteristic method lines terminate in a stable shock wave but do not emanate from it (Lev et al., 1986). It should be stated that it is well established that the entropy condition is equivalent to the viscous profile or the diffusion term used earlier. That is the generalized entropy condition solution is proved to be the limit of the equation with a small diffusion term (Chancelier et al. 1994). Fig. 3 shows an example of a stable and a non-stable discontinuity in a batch flux curve. The speed of the discontinuity is given by the Rankine–Hugoniot condition (Oleinik, 1960, 1963) as follows:

$$v_d = \frac{f(c(x^+)) - f(c(x^-))}{c(x^+) - c(x^-)}. \tag{12}$$

Discontinuities satisfying Eqs. (11) and (12) are known as *shocks*. If the *shock* chord of Eq. (12) is tangential to the flux curve at $c(x^+)$ or $c(x^-)$, then the *shock* is further described as a *contact discontinuity*.

Another known phenomena is the *rarefaction wave* at which a discontinuity would not be stable and no shocks will form. *Rarefaction wave*s occur when the slope of the flux at any point between $c(x^-)$ and $c(x^+)$ is always negative (positive) for $c(x^-)$ less (greater) than $c(x^+)$. At such condition the Riemann problem will resolve to a continuous solution. For example, if the two points c_2^- and c_2^+ in Fig. 4 represent initial concentrations above and below a certain height x of the settler, respectively, then at time > 0 a rarefaction wave will develop and give a continuous concentration gradient between the two concentrations.

2.6. Polydisperse sedimentation model

Extending the last section to the simulation of polydisperse suspension requires further modification and discussion. Using a settling velocity model based on the particle size and density will produce different flux curves for each suspension quality and each particle type, resulting in different behaviour among particles of different sizes and densities in the sedimentation process. Some particles might cause overloading and exit at the bottom and the top. At the same time, different particle types might be efficiently removed.

Assuming we have a suspension of particles that consist of different sizes and densities, we define the kth particle as a particle with a unique size and density in a suspension of l different particle types, where $k = 1, 2, 3, \ldots, l$. Consequently,

the partial differential equation is re-written as follows:

$$\frac{\partial}{\partial t}\begin{bmatrix} c_1(x) \\ c_2(x) \\ \vdots \\ c_k(x) \\ \vdots \\ c_l(x) \end{bmatrix} + \frac{\partial}{\partial x}\begin{bmatrix} f(c_1(x)) \\ f(c_2(x)) \\ \vdots \\ f(c_k(x)) \\ \vdots \\ f(c_l(x)) \end{bmatrix} = \begin{bmatrix} s_1(t) \\ s_2(t) \\ \vdots \\ s_k(t) \\ \vdots \\ s_l(t) \end{bmatrix} \delta(x), \tag{13}$$

where $c_k(x)$ is the kth particle concentration at height x.

2.7. Numerical simulation

The treatment of fluid dynamics and sedimentation problems with shocks is a complicated mathematical subject. By using the theory of analytical solution, one can derive numerical algorithms that automatically take the entropy condition into account. Lax and Wendroff (1960) and Lax (1957) have shown that such schemes satisfy the jump condition across a discontinuity, thus, the entropy condition is part of the numerical simulation. In general, there are three classes of schemes for handling discontinuities as shown by Press et al. (2002). The simplest method is to add an artificial viscosity term to the mass balance, which would smooth the discontinuity. A second method applies a high-order differencing scheme that is accurate for smooth regimes and a low-order dissipative scheme that can smooth the shocks. The third and potentially most powerful scheme is the Godunov (1959) approach. The scheme does not use the typical linearization approach based on Taylor series expansion as the previous finite differencing schemes have done. Instead, Godunov's scheme explicitly includes the non-linearity of the mass balance equations. The Riemann shock problem is known for its analytical solution for two uniform states of fluid separated by a discontinuity. Godunov approximated the fluid by a large number of cells brought together using the Riemann problem. Several papers generalized the Godunov approach to suit the system they described. Diehl (1997) provided a generalization of the Godunov approach to the entire settler including discontinuous conditions at feed point and the two outlets.

Diehl has provided additional entropy condition for the stationary discontinuities of the input and the two outlets, where such discontinuity has a speed of zero. Diehl's work provided the scheme to simulate the entire settler.

In order to perform the simulation, a Godunov finite-difference scheme is used to solve the mass balance, where Δt is the temporal grid size and Δx is the spatial grid size. First, the distance grid points $i = 2,\ldots,n-1$ are updated according to following algorithm, where i index stands for the distance space grid and j stands for the time space grid:

$$c_i^{j+1} = c_i^j + \frac{\Delta t}{\Delta x}(G_{i-1/2}^j - G_{i+1/2}^j),$$
$$i = 2,\ldots,m-1, \tag{14}$$

$$c_m^{j+1} = c_m^j + \frac{\Delta t}{\Delta x}(G_{i-1/2}^j - F_{i+1/2}^j + S^j),$$
$$i = m, \tag{15}$$

$$c_i^{j+1} = c_i^j + \frac{\Delta t}{\Delta x}(F_{i-1/2}^j - F_{i+1/2}^j),$$
$$i = m+1,\ldots,n-1, \tag{16}$$

where

$$S^j = \frac{Q_f^j c_f^j}{A}, \tag{17}$$

$$G_{i-1/2}^j = \begin{cases} \min\limits_{c_{i-1}^j \leqslant c \leqslant c_i^j} g(c) & c_{i-1}^j \leqslant c_i^j, \\ \max\limits_{c_i^j \leqslant c \leqslant c_{i-1}^j} g(c) & c_{i-1}^j > c_i^j, \end{cases} \tag{18}$$

where Q_f is the feed-flow rate, u_f is the feed concentration. Similar equations like Eq. (18) are developed for $G_{i+1/2}^j$, $F_{i-1/2}^j$, and $F_{i+1/2}^j$.

Output and boundary values at $i=1$ and $i=n$ are calculated according to the following:

$$c_1^{j+1} = \begin{cases} c_2^{j+1} & c_2^{j+1} \in (c_z, c_{\max}], \\ 0 & c_2^{j+1} \in [0, c_z], \end{cases} \tag{19}$$

$$c_e^{j+1} = c_1^{j+1} - \frac{f_b(c_1^{j+1})}{v_{f,e}}, \tag{20}$$

$$c_n^{j+1} = \begin{cases} c_{n-1}^{j+1} & c_{n-1}^{j+1} \in [0, c_m) \cup (c_M, c_{\max}], \\ c_M & c_{n-1}^{j+1} \in [c_m, c_M], \end{cases} \tag{21}$$

$$c_u^{j+1} = c_n^{j+1} + \frac{f_b(c_n^{j+1})}{v_{f,u}}, \tag{22}$$

where c_z and c_M are local minimizers of the flux functions $f(c)$ and $g(c)$, respectively, c_e is the overflow (effluent) concentration and c_u is the underflow concentration. The c_m limitation is the value strictly less than c_M that satisfies $f(c_m) = f(c_M)$. Such concentration conditions at the bottom and the top layers fits the criteria of stable discontinuities discussed earlier using the Reimann problem approach and a discontinuity of zero speed (Diehl, 1996). Conditions at the boundaries of the settler serve a critical rule in determining the dynamics at $x < D$ and $x > D$. Eqs. (19)–(22) represent calculation of fluxes at outlets using the entropy condition introduced by Diehl (1996, 1997), where stable values are picked to represent fluxes at these distance grid points.

The minimum and maximum conditions replaces the minimal conditions used by earlier researchers based on 'experience', which were mentioned earlier in the review section. The minimum and maximum conditions ensures that a stable discontinuity is picked and unstable discontinuities rejected. For example, if concentration at stage i is lower than concentration at stage $i+1$, and flux function predicts a local minimum between the fluxes of the two stages, then the local minimum flux should be used in the calculations because the chord between the two fluxes at the two stages is above the flux curve, which is an unstable discontinuity.

Adding the concept of polydisperse suspension with l particle types ($k = 1, 2, 3, \ldots, l$), the above equations would be modified as follows:

$$\begin{bmatrix} c_{1,i}^{j+1} \\ c_{2,i}^{j+1} \\ \vdots \\ c_{l,i}^{j+1} \end{bmatrix} = \begin{bmatrix} c_{1,i}^{j} \\ c_{2,i}^{j} \\ \vdots \\ c_{l,i}^{j} \end{bmatrix} + \frac{\Delta t}{\Delta x} \left(\begin{bmatrix} G_{1,i-1/2}^{j} \\ G_{2,i-1/2}^{j} \\ \vdots \\ G_{l,i-1/2}^{j} \end{bmatrix} - \begin{bmatrix} G_{1,i+1/2}^{j} \\ G_{2,i+1/2}^{j} \\ \vdots \\ G_{l,i+1/2}^{j} \end{bmatrix} \right), \quad (23)$$

$i = 2, \ldots, m-1,$

where,

$$\begin{bmatrix} S_1^j \\ S_2^j \\ \vdots \\ S_l^j \end{bmatrix} = \frac{Q_f^j}{A} \begin{bmatrix} c_{1,f}^{j} \\ c_{2,f}^{j} \\ \vdots \\ c_{l,f}^{j} \end{bmatrix}, \quad (24)$$

$$G_{k,i-1/2}^{j} = \begin{cases} \min\limits_{c_{k,i-1}^{j} \leqslant c \leqslant c_{k,i}^{j}} g(c) & c_{k,i-1}^{j} \leqslant c_{k,i}^{j}, \\ \max\limits_{c_{k,i}^{j} \leqslant c \leqslant c_{k,i-1}^{j}} g(c) & c_{k,i-1}^{j} > c_{k,i}^{j}. \end{cases} \quad (25)$$

Similar equations like Eq. (25) are developed for $G_{k,i+1/2}^{j}$, $F_{k,i-1/2}^{j}$, and $F_{k,i+1/2}^{j}$.

Output and boundary values at i=1 and i=n are calculated according to the following:

$$c_{k,1}^{j+1} = \begin{cases} c_{k,2}^{j+1} & c_{k,1}^{j+1} \in (c_{k,z}, c_{k,\max}], \\ 0 & c_{k,1}^{j+1} \in [0, c_{k,z}], \end{cases} \quad (26)$$

$$\begin{bmatrix} c_{1,e}^{j+1} \\ c_{2,e}^{j+1} \\ \vdots \\ c_{l,e}^{j+1} \end{bmatrix} = \begin{bmatrix} c_{1,1}^{j+1} \\ c_{2,1}^{j+1} \\ \vdots \\ c_{l,1}^{j+1} \end{bmatrix} - \frac{1}{v_{f,e}} \begin{bmatrix} f_b(c_{1,1}^{j+1}) \\ f_b(c_{2,1}^{j+1}) \\ \vdots \\ f_b(c_{l,1}^{j+1}) \end{bmatrix}, \quad (27)$$

$$c_{k,n}^{j+1} = \begin{cases} c_{k,n-1}^{j+1} & c_{k,n-1}^{j+1} \in [0, c_{k,m}) \cup (c_{k,M}, c_{k,\max}], \\ c_{k,M} & c_{k,n-1}^{j+1} \in [c_{k,m}, c_{k,M}], \end{cases} \quad (28)$$

$$\begin{bmatrix} c_{1,u}^{j+1} \\ c_{2,u}^{j+1} \\ \vdots \\ c_{l,u}^{j+1} \end{bmatrix} = \begin{bmatrix} c_{1,n}^{j+1} \\ c_{2,n}^{j+1} \\ \vdots \\ c_{l,n}^{j+1} \end{bmatrix} + \frac{1}{v_{f,u}} \begin{bmatrix} f_b(c_{1,n}^{j+1}) \\ f_b(c_{2,n}^{j+1}) \\ \vdots \\ f_b(c_{l,n}^{j+1}) \end{bmatrix}. \quad (29)$$

As shown above, each component mass balance at space stage j and distance stage i is calculated independently. But the basic constitutive variable, which is the settling velocity, is calculated based on the suspension present in the system. The settling velocity of the kth particle is calculated at distance grid i and time j using the proper interaction and hydrodynamic settling velocity equation in a suspension of different particles. In other words, even though the equations seem independent of each other, the settling velocity calculated for each species is dependent on each other. This ensures that the effect of hindered settling is taken into consideration.

2.8. Multi-components flux curves

The numerical methodology used in our paper raises new concepts in the application of the flux curve. The original work of Diehl using Godunov numerical scheme uses a single fixed flux curve for modelling the whole settler including outlets. Such a flux curve is obtained experimentally when designing settlers and determining parameters of flux-based settling velocity models. On the other hand, in our simulation, the settling flux curve is not constant in shape and keeps changing dynamically. As a matter of fact, a different flux curve is obtained for each particle type in the suspension. In addition, a flux curve of a certain particle in monodispersed suspension will not have the same flux curve shape if that same particle type was present in a multi-particle suspension. Furthermore, in dynamic simulation, the flux curve of a certain particle will be changing dynamically at different layers since the suspension concentration and quality will change continuously. Also, the flux curve at each height will keep changing with time as the suspension quality and particles concentrations change in a dynamic manner. The implication of such modelling is powerful since it has the ability to determine which

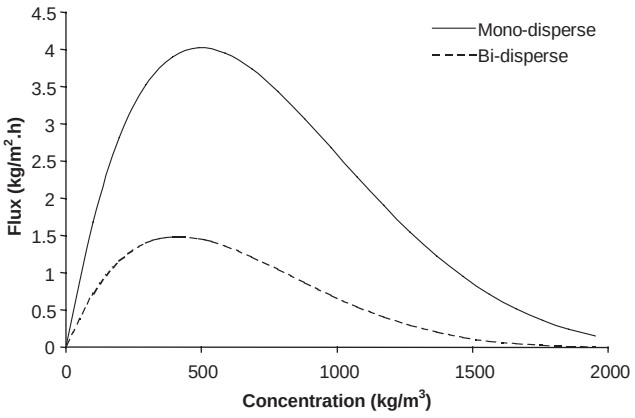

Fig. 5. Batch flux curve of large solids (diameter = 0.496 mm and density = 2790 kg/m^3) in monodisperse suspension and bidisperse suspension (with small solids of diameter = 0.125 mm and the same density at a concentration of 558 kg/m^3).

particles will be overloading and which particles will settle. This eliminates the need for any imposed criterion to determine the overflow concentrations and particle-size distribution. Also, the simulation eliminates the need for two different models to describe the system: one describing the thickening process and the other the overflow based on feed conditions. Fig. 5 shows an example of batch flux curve of large solids (diameter = 0.496 mm and density = 2790 kg/m^3) in a monodisperse suspension and bidisperse suspension (with small solids of diameter = 0.125 mm and the same density at a concentration of 558 kg/m^3). The liquid medium used had a density of 1208 kg/m^3 and viscosity of 0.02416 kg/m/s. The settling velocity model used was that of Richardson and Zaki coupled with Masliyah correlation.

In our simulation, the average concentrations between the two stages for all existing particles were used to approximate the flux curve between these stages. Then, the obtained flux curve is used to calculate the flux between the two stages whenever it is required by the numerical scheme shown earlier. The minimum local point c_M of the flux is calculated using the golden section search scheme combined with Brent's method. The scheme uses Brent's method of finding a minimum or maximum using three points for parabolic interpolation. When the Brent's method is not cooperative such as in the case when the three points are colinear, the simulation switches to the slow and guaranteed golden section method. Root finding is performed using the secant method, which is a faster method than the bisection and the false position methods for smooth roots. Smooth roots is thought to be the typical case for finding the points c_z and c_m, thus, other search engines such as Ridder's method and Brent's method were not required.

2.9. Steady-state solutions

Based on the paper by Diehl (2001), steady-state solution was determined by operation charts of flux curves. The location of the feed concentration and feed flux in the flux curve determined the steady-state solution. The reader is referred to that paper for further details. A problem in our simulation is that our flux curves are continuously changing depending on the feed-flow conditions. The feed-flow flux curve is different than the flux curve inside the settler. The flux curve inside the settler might be different from one stage to another.

An approximated solution to the problem was obtained by first using the feed flux curve to construct the steady-state solution inside the settler. Then, a stage inside the settler and below the feed point that contains a concentration profile is used to construct the steady-state solution and overwrite the current profile. Re-construction of the internal solution was repeated using internal concentration profile until the mass balance of input and outputs converges to a proper solution within a selected tolerance limit. But a problem might still exist because in dynamic mode, calculations at each stage including at the outputs depend on the local flux curve while in the steady-state calculations, solution depends on a flux curve at a single stage to represent the whole settler. This difference will cause some discrepancy at the overflow of the settler between steady-state and dynamic mode calculations for certain cases depending on how different are the two flux curves: the flux curve at the top and the flux curve used to perform the steady-state calculations. No problem will be present in the underflow since the flux curve used in the steady state calculation is from the *thickening zone*.

3. Case studies

The paper by Bürger et al. (2000c) presented simulation of multi-particle suspensions and provided many interesting and critical cases to examine. The same ideas were used with the presented model using 3D graphs on the contrary to their graphs. We have also simulated a continuous settler case while their paper was limited to the batch simulation. Nevertheless, we believe that their paper provided an insightful presentation of multi-particle suspension simulation and the reader is encouraged to review it along with this paper. We have used Richardson and Zaki model coupled with Masliyah equation, which have shown a better fit with experimental data (Zeidan et al., 2003a).

3.1. Batch column settling test

Due to the lack of experimental data for the sedimentation of multi-particles in a wastewater treatment settler unit, comparison with experimental data of settling tests is justified. The first case presented is the one simulated by Bürger et al. (2000c) of bidisperse suspension of two glass beads of different sizes ($d_1 = 0.496$ and $d_2 = 0.125$ mm) and the same density ($\rho = 2790$ kg/m^3). The liquid medium was of a density of 1208 kg/m^3 and viscosity of 0.02416 kg/m/s. The initial concentrations were $c_1 = 558$ kg/m^3 and

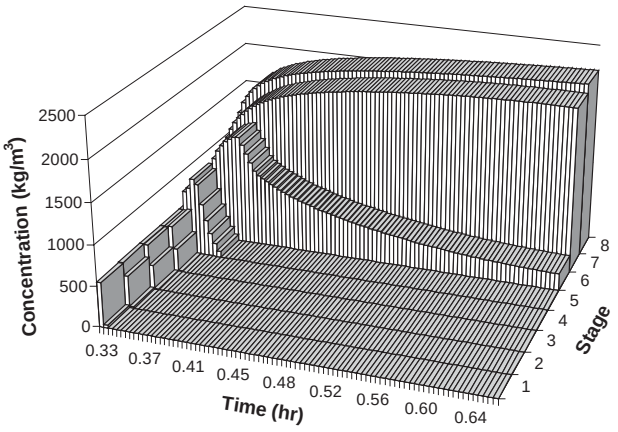

Fig. 6. Settling of bidisperse suspension of heavy particles of two sizes: large particles (diameter = 0.496 mm) concentration vs. stage number and time. Initial conditions: large particles concentration = 558 kg/m^3 and small particles concentration = 139.5 kg/m^3.

c_2 = 139.5 kg/m^3 for large and small particles, respectively, in a well-mixed settling column of a height of 0.3 m. The simulation duration was for 0.33 h and the settler was divided into eight stages plus two stages (0 and 9) for boundary conditions. Stage 1 is the top of the settler and stage 8 is the bottom.

Results shown in Fig. 6 show that large solids settled down to the bottom of the settler as expected. Thickened sediment of large solids started to build up at the bottom stage, followed by the same behaviour in the seventh stage. The large solids concentration in the sixth stage initially started to increase until no more large particles were present in the upper stages. At that point, the concentration in stage 7 started to decrease because large particles continued to settle to stage 8 and occupy available spaces.

Fig. 7a shows that the concentrations of small particles decreased in all stages and increased at the intermediate stage 5. The small particles from stages 1 to 4 settled downward as expected, but particles in stages 6–8 moved upward. The settling of large solids to the bottom pushed the small solids upward. When the concentration of large solids at stage 6 started to decrease, more space in that stage became available for small particles to occupy. Thus, the small particles started to move from stages 5 to 6 resulting in a smooth slow reduction of small solids concentration in the fifth stage and an increase of small solids concentration in the sixth stage as shown in Fig. 7b. Eventually, most of the large particles would occupy the bottom stages and a layer or two of mostly small particles would cover the large ones. The simulation was similar to the results obtained by Bürger et al. (2000c) (Fig. 2). Also, the graphs presented the flexibility of hydrodynamic models in comparison to the flux-based models, which usually simulate the combination or summation of the Figs. 6, 7a and b and do not distinguish between the two particle sizes.

Another observation is that stage 1 indicates that it initially increased in concentration as if the small particles initially moved upward because of the presence of large particles in the same zone. As soon as the large particles left the region to the bottom of the column, concentrations of small particles at the above stages started to decrease indicating that small particles started to settle downward. Such observation was also obvious in the paper by Bürger et al. (2000c) (Fig. 3).

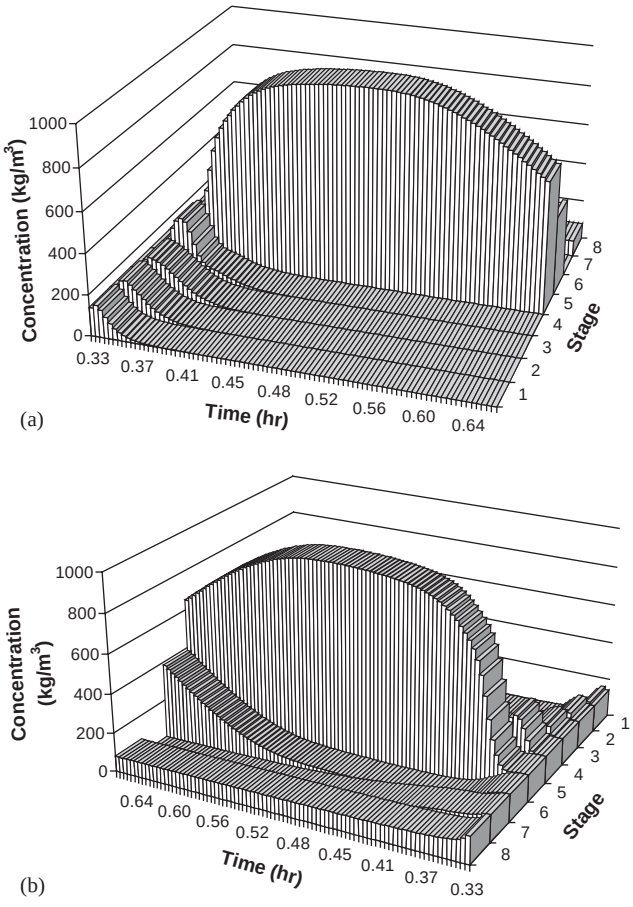

Fig. 7. (a and b) Settling of bidisperse suspension of heavy particles of two sizes: small particles (diameter = 0.125 mm) concentration vs. stage number and time. Initial conditions: large particles concentration = 558 kg/m^3 and small particles concentration = 139.5 kg/m^3.

3.2. Rarefaction waves

Two examples that were expected to produce rarefaction waves were used here to examine the ability of our simulation to predict them. The two examples were constructed using the same particles and liquid medium shown in case 3.3.1 and the same settling velocity model. In the first example, the upper sections of the column were occupied with a bidisperse suspension of particles at initial concentrations of 279 kg/m^3 for each particle type. The lower half of the column was occupied by pure liquid. Fig. 8 shows how large particles have fallen downward rapidly to occupy the bottom layer of the settler.

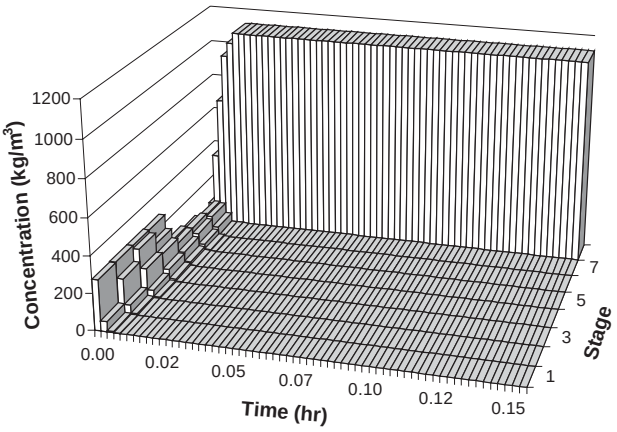

Fig. 8. Settling of bidisperse suspension of heavy particles of two sizes: large particles (diameter = 0.496 mm) concentration vs. stage number and time. Initial conditions: large particles concentration = 279 kg/m^3 and small particles concentration = 279 kg/m^3 at the upper half.

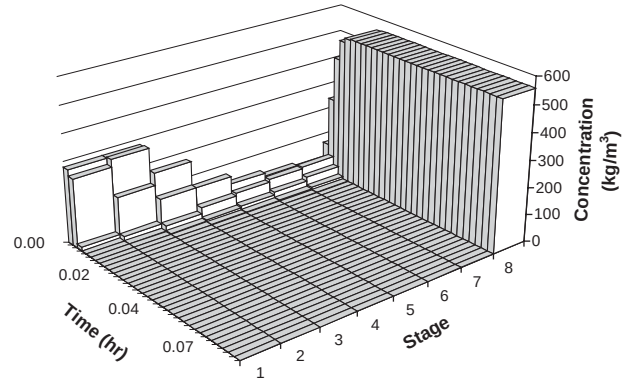

Fig. 10. Settling of bidisperse suspension of heavy particles of two sizes: large particles (diameter = 0.496 mm) concentration vs. stage number and time. Initial conditions: large particles concentration = 279 kg/m^3 at the upper quarter and small particles concentration = 279 kg/m^3 at the upper second quarter.

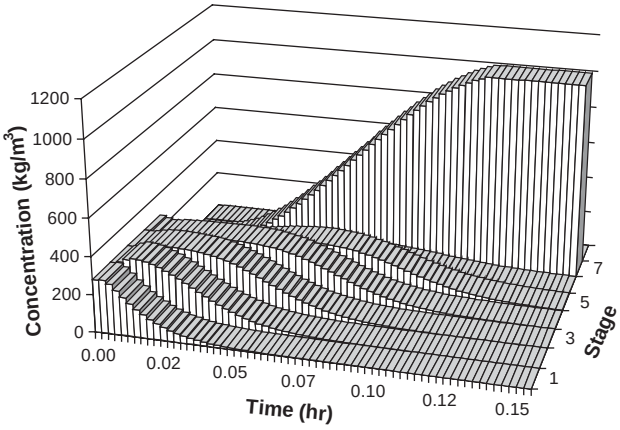

Fig. 9. Settling of bidisperse suspension of heavy particles of two sizes: small particles (diameter = 0.125 mm) concentration vs. stage number and time. Initial conditions: large particles concentration = 279 kg/m^3 and small particles concentration = 279 kg/m^3 at the upper half.

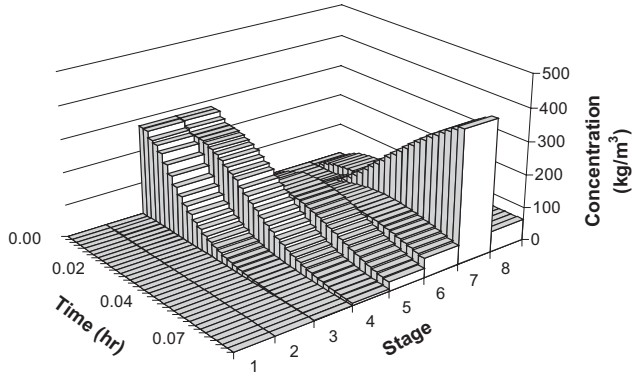

Fig. 11. Settling of bidisperse suspension of heavy particles of two sizes: small particles (diameter = 0.125 mm) concentration vs. stage number and time. Initial conditions: large particles concentration = 279 kg/m^3 at the upper quarter and small particles concentration = 279 kg/m^3 at the upper second quarter.

At the first time slot in Fig. 8, large particles at initial conditions are shown in the upper stages of the column. At the second time slot, the concentrations at these stages decreased. It was noted that the reductions of concentrations were not equal in value among the four stages. Concentration in stage 1 observed the highest reduction, then the second stage then the third. The varying concentration changes represented different large particles settling velocities at different stages. This indicated that the presence of small particles has slowed the settling velocity of large particles. At stage 4, the settling velocity of large particles seems slow but slightly faster than the one in stage 3. The reason was that slowly settling small particles have not reached stage 5 significantly giving large particles the chance to transfer from stages 4 to 5 faster. In fact, looking at Fig. 9, stages 1–4 show a varying increase of concentration of small particles in each stage demonstrating that they initially moved upward due to the settling of large particles through the same zone.

As the small particles settled down, they continued to expand their partial and complete bill-like concentration distribution with time and distance. The change of bill-like shape, which was decreasing in height and spreading in width from one stage to a lower stage, indicated the formation of rarefaction waves. A close look revealed that the same trend was observed for large particles as they travelled through the small particles zone and continued to the bottom of the column.

In the second example, the large particles initially occupied the upper quarter of the column at a concentration of 279 kg/m^3 and the small particles occupied the second upper quarter at the same concentration. Figs. 10 and 11 indicate how the large particles settled faster and overcame the small particles to reach the bottom of the settler. Fig. 11

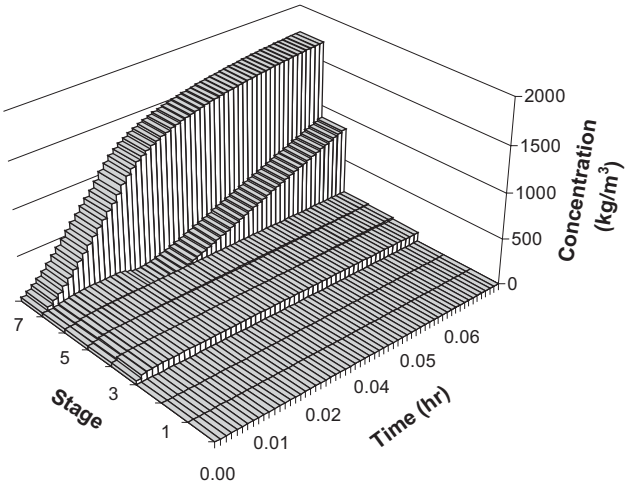

Fig. 12. Continuous sedimentation of bidisperse suspension of heavy particles of two sizes starting at steady state with a feed flow rate jump of 0.1 m^3/h: large particles (diameter = 0.496 mm) concentration vs. stage number and time.

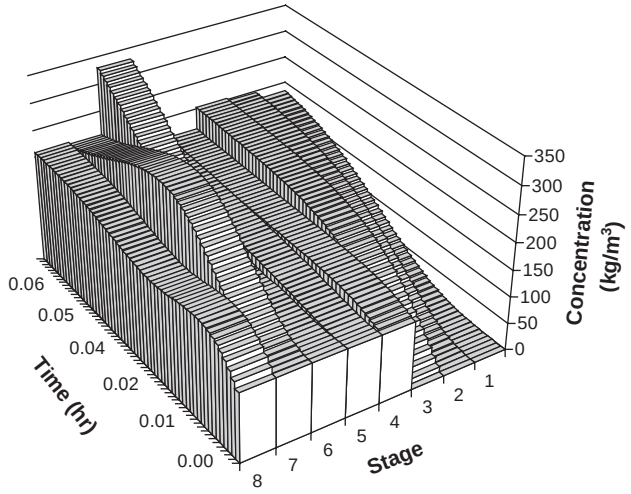

Fig. 13. Continuous sedimentation of bidisperse suspension of heavy particles of two sizes starting at steady state with a feed flow rate jump of 0.1 m^3/h: small particles (diameter = 0.125 mm) concentration vs. stage number and time.

shows stage 4 in the time frame 0–0.02 hours, in which the small particles initially started settling in a fast rate (indicated by the reduction of concentration with the progress of time). But they rapidly started to slow down due to the passage of large particles as indicated by the reducing change of concentration with time. As soon as the large particles left the small particles zone, the settling velocity of small particles started to speed up again. Such behaviour was also captured by Bürger et al. (2000c) (Fig. 19). Small particles finally settled at the bottom of the column. Most of the small particles occupied the seventh stage, while a small quantity managed to settle in the left unoccupied space of the eighth stage. Again, the continuous increase of the width and decrease of the height of the partial and complete bill-like shape of the suspension distribution with time and distance indicated the formation of a rarefaction wave.

3.3. Continuous settling column

A hypothetical case was simulated using the same suspension of the previous examples and assuming a column diameter 0.2 m, input flow rate of 0.1 m^3/h and outputs flow rates of 0.05 m^3/h each. The simulation of the sedimentation column starting from a steady-state solution and handled a feed jump from 0.1 to 0.2 m^3/h for a period of 0.07 hours.

The input jump of flow rate has prompted the build up of a thickened blanket of large particles, which started to grow at stage 8 and continued to the seventh stage as shown in Fig. 12. Meanwhile, small particles showed turbulent behaviour as seen in Fig. 13. Initially and because of the feed flow jump, concentration of small particles at the eighth stage started to increase, but due to the rapid increase of large solids concentration at the same stage, small particles started to move upward towards the seventh stage. The trend continued and small particles at the seventh stage started to move upward as more large solids settled down. Thus, the settler could not handle higher volume of small particles at the feed and the concentration of small particles at the upper stages started to increase, which might cause an overflow with small particles. The figures show that the simulation predicted the rapid build up of small particles in the upper stages, which would affect the effluent stream in this particular case, while large particles still building up at the bottom stages of the settler.

3.4. Light and heavy particles

To simulated the effect of the presence of two particles, one with a density heavier than that of the fluid and the other of a density lighter than the fluid, a binary suspension was constructed. The heavy particles were of a density of 1186 kg/m^3 and the light particles had a density of 1050 kg/m^3. The fluid density was 1120 and the viscosity was 0.000141 kg/m/s. Richardson and Zaki model was used for the simulation with a settler divided into 10 stages including the boundary condition stages. The vessel simulated was 0.3 m in height and the initial concentration in the well-mixed column was 94.9 and 84.0 kg/m^3 for heavy and light solids, respectively.

The results in Figs. 14 and 15 predicted correctly the separation of the two particle types, where heavy particles settled down and light buoyant particles travelled to the surface. Examining both figures at the middle stages, we can confirm the observation by Bürger et al. (2000c) that the two particles completely separate after about 0.05 hours.

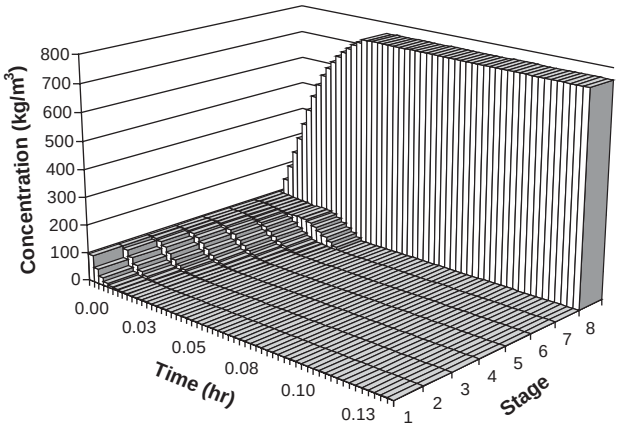

Fig. 14. Settling of bidisperse suspension of heavy and light particles of single size (0.125 mm): Heavy particles (density = 1186 kg/m^3) concentration vs. stage number and time. Initial conditions: heavy particles concentration=94.9 kg/m^3 and light particles concentration=84.0 kg/m^3.

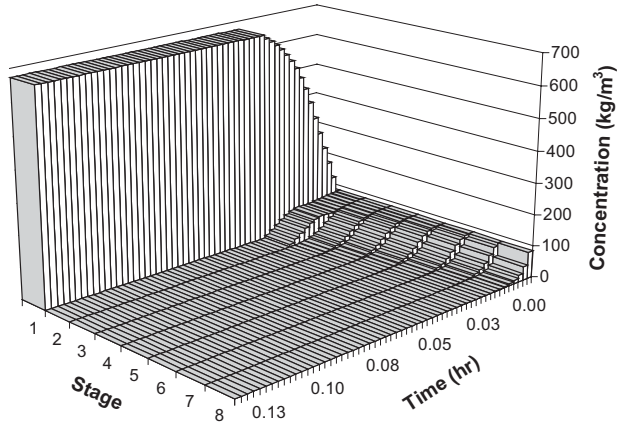

Fig. 15. Settling of bidisperse suspension of heavy and light particles of single size (0.125 mm): Light particles (density = 1050 kg/m^3) concentration vs. stage number and time. Initial conditions: heavy particles concentration=94.9 kg/m^3 and light particles concentration=84.0 kg/m^3.

3.5. Other cases

The reader is also directed to other simulated cases of the settler combined with other processes such as the activated sludge process. A steady-state simulation of the activated sludge process is shown by Zeidan et al. (2003b).

4. Conclusion

Simulation of polydisperse suspension was accomplished successfully using the Godunov classical numerical method and hydrodynamic non fluxed-based settling velocity models. The simulation eliminated the need for separate models to describe the overflow based on the feed information. It also replaced imposed parameters and threshold values required in earlier simulations to describe effluent concentrations of settling and non-settling particles. Also, the numerical simulation presented in this paper provided the capability of predicting particle size distribution at both output streams of the settler unit.

Notation

A	cross sectional area of the settler, length^2
D	thickening zone depth or batch settler depth, length
c	concentration of particles, mass/length^3
$c(x)$	concentration at settler height x, length
c_e	concentration of the effluent (overflow) stream, mass/length^3
c_f	feed concentration mass/length^3,
c_k	concentration of the kth particle type, mass/length^3
$c_k(x)$	kth particle concentration at height x, mass/length^3
c_i	concentration at distance space grid I, mass/length^3
c^j	concentration at time space grid j, mass/length^3
c_m	value strictly smaller than c_M that satisfies $f(c_m) = f(c_M)$, mass/length^3
c_M	local minimizer of the flux function $g(c)$, mass/length^3
c_{max}	maximum attainable concentration, mass/length^3
c_o	initial homogeneous suspension concentration, mass/length^3
c_u	concentration of the underflow stream, mass/length^3
c_z	local minimizer of the flux function $f(c)$, mass/length^3
f	subscript denoting feed
$f(c)$	downward flux function, mass/length^2/time
$f(c(x))$	flux function, mass/length^2/time
$f_b(c)$	batch flux function, mass/length^2/time
$f_b(c(x))$	batch flux function, mass/length^2/time
F	Godunov downward flux function, mass/length^2/time
$g(c)$	upward flux function, mass/length^2/time
G	Godunov upward flux function, mass/length^2/time
H	clarification section height, length
i	distance space grid
j	time space grid
k	particle type index in a suspension of l particles
l	number of particles types
L	depth of the sedimentation tank, length
m	feed space grid index
min	minimum between two points
max	maximum between two points
n	number of stages of distance space grids
Q_e	the overflow flow rate, length^3/time

Q_f	the feed flow rate, length^3/time
Q_u	the underflow flow rate, length^3/time
S	feed or source flux, mass/length/time
$s(t)$	source or feed function
t	time time
$v_{f,u}$	bulk velocity of the underflow, length/time
$v_{f,e}$	bulk velocity of the effluent, length/time
v_s	the particle settling velocity due to gravity, length/time
$\delta(x)$	delta function.

Acknowledgements

The authors wish to acknowledge useful discussions with Dr. P. Whiting and Dr. R. Farnood.

References

Barnea, E., Mizrahi, J., 1973. A generalized approach to the fluid dynamics of particulate systems, part I: general correlation for fluidization and sedimentation in solid multiparticle systems. Chemical Engineering Journal 5, 171–189.

Bürger, R., Concha, F., 1998. Mathematical model and numerical simulation of the settling of the flocculated suspensions. International Journal of Multiphase Flow 24, 1005–1024.

Bürger, R., Bustos, M.C., Concha, F., 1999. Settling velocities of particulate systems: 9. Phenomenological theory of sedimentation processes: numerical simulation of the transient behaviour of flocculated suspensions in an ideal batch or continuous thickener. International Journal of Mineral Processing 55, 267–282.

Bürger, R., Concha, F., Tiller, F.M., 2000a. Applications of the phenomenological theory to several published experimental cases of sedimentation processes. Chemical Engineering Journal 80, 105–117.

Bürger, R., Evje, S., Karlsen, K.H., Lie, K.-A., 2000b. Numerical methods for the simulation of the settling of flocculated suspensions. Chemical Engineering Journal 80, 91–104.

Bürger, R., Concha, F., Fjelde, K.-K., Karlsen, K.H., 2000c. Numerical simulation of the settling of polydisperse suspensions of spheres. Powder Technology 113, 30–54.

Bürger, R., Fjelde, K.-K., Höfler, K., Karlsen, K.H., 2001. Central difference solutions of the kinematic model of settling of polydisperse suspensions and three-dimensional particle-scale simulations. Journal of Engineering Mathematics 41, 167–187.

Bustos, M.C., Concha, F., Wendland, W.L., 1990. Global weak solutions to the problem of continuous sedimentation of an ideal suspensions. Mathematical Methods in the Applied Sciences 13, 1–22.

Chancelier, J.P., Cohen De Lara, M., Pacard, F., 1994. Analysis of a conservation pde with discontinuous flux: a model of settler. SIAM Journal of Applied Mathematics 54 (4), 954–995.

Cho, S.H., Colin, F., Sardin, M., Prost, C., 1993. Settling velocity model of activated sludge. Water Research 27 (7), 1237–1242.

Concha, Bustos, 1987. A modification of the Kynch theory of sedimentation. A.I.Ch.E. Journal 33(2), 312–315.

Chueng, M.K., Powell, R.P., McCarthy, M.J., 1996. Sedimentation of noncolloidal bidisperse suspensions. A.I.Ch.E. Journal 43 (1), 271–276.

Dallavalle, J.M., 1948. Micromeritics. Pitman, London.

Diehl, S., 1995. On scalar conservative laws with point source and discontinuous flux function. SIAM Journal on Mathematical Analysis 26 (6), 1425–1451.

Diehl, S., 1996. A conservative law with point source and discontinuous flux function modelling continuous sedimentation. SIAM Journal of Applied Mathematics 56 (2), 338–419.

Diehl, S., 1997. Dynamic and steady-state behavior of continuous sedimentation. SIAM Journal of Applied Mathematics 57 (4), 991–1018.

Diehl, S., 2001. Operating charts for continuous sedimentation I: control of steady states. Journal of Engineering Mathematics 41, 117–144.

Diehl, S., Jeppsson, U., 1998. A model of the settler coupled to the biological reactor. Water Research 22 (2), 331–342.

Doheim, M.A., Abu-Ali, M.H., Mabrouk, S.A., 1997. Investigation and modelling of sedimentation of mixed particles. Powder Technology 91, 447.

Dupont, R., Henze, M., 1992. Modelling of the secondary clarifier combined with the activated sludge model no. 1. Water Science and Technology 25 (6), 285–300.

Font, R., Ruiz, F., 1993. Simulation of batch and continuous thickeners. Chemical Engineering Science 48 (11), 2039–2047.

Garrido, P., Bürger, R., Concha, F., 2000. Settling velocities of particulate systems: 11. Comparison of the phenomenological sedimentation-consolidation model with published experimental results. International Journal of Mineral Processing 60, 21227.

Garside, J., Al-Dibouni, M.R., 1977. Velocity–voidage relationship for fluidization and sedimentation in solid–liquid system. Industrial and Engineering Chemistry Process Design and Development 16, 206.

Godunov, S.K., 1959. A finite difference method for the numerical computations of discontinuous solutions of the equations of fluid dynamics. Matematicheski Sbornik 47, 271–306.

Grijspeerdt, K., Vanrolleghem, P., Verstraete, W., 1995. Selection of one-dimensional sedimentation: models for on-line use. Water Science and Technology 31 (2), 19204.

Hamilton, J., Jain, R., Antoniou, P., Svoronos, S.A., Koopman, B., Lyberatos, G., 1992. Modeling and pilot-scale experimental verification for predenitrification process. Journal of Environmental Engineering 118 (1), 38–55.

Härtel, L., Pöpel, H.J., 1992. A dynamic secondary clarifier model including processes of sludge thickening. Water Science and Technology 25 (6), 267–284.

Jeppsson, U., Diehl, S., 1996. An evaluation of a dynamic model of the secondary clarifier. Water Science and Technology 34 (5–6), 19–26.

Kynch, G.J., 1952. A theory of sedimentation. Transactions of the Faraday Society 48, 166–176.

Lax, P.D., 1957. Hyperbolic systems of conservation laws. II. Communications on Pure and Applied Mathematics 10, 537–566.

Lax, P.D., Wendroff, B., 1960. Systems of conservation laws. Communications on Pure and Applied Mathematics 13, 217–237.

Lev, O., Rubin, E., Sheintuch, M., 1986. Steady state analysis of a continuous clarifier-thickener system. A.I.Ch.E. Journal 32 (9), 1516–1525.

Lockett, M.J., Al-Habbooby, H.M., 1973. Differential settling by size of two particle species in a liquid. Transactions of the Institution of Chemical Engineers 51, 281–292.

Masliyah, J.H., 1979. Hindered settling in a multi-species particle system. Chemical Engineering Science 34, 1166–1168.

Mazzolani, G., Pirozzi, F., d'Antonoi, G., 1998. A generalized settling approach in the numerical modeling of sedimentation tanks. Water Science and Technology 38 (3), 95–102.

Mirza, S., Richardson, J.F., 1978. Sedimentation of suspensions of particles of two or more sizes. Chemical Engineering Science 34, 447–454.

Otterpohl, R., Freund, M., 1992. Dynamic models for clarifiers of activated sludge plants with dry and wet weather flows. Water Science and Technology 26 (5–6), 1391–1400.

Oleinik, O.A., 1960. Uniqueness and stability of the generalized solution of Cauchy problem for a quasi-linear equation. American Mathematical Society Translations 33 (2), 285–290.

Oleinik, O.A., 1963. Discontinuous solutions of nonlinear differential equations. American Mathematical Society Translations 26 (2), 95–172.

Patwardhan, V.S., Tien, C., 1985. Sedimentation and liquid fluidization of solid particles of different sizes and densities. Chemical Engineering Science 40 (7), 1051–1060.

Petty, C.A., 1975. Continuous sedimentation of a suspension with a nonconvex flux law. Chemical Engineering Science 30, 1451–1458.

Press, W.H., Teukolsky, S.A., Vetterling, W.T., Flannery, B.P., 2002. Numerical Recipes in C++. Cambridge University Press, New York, NY.

Quispe, J., Concha, F., Toledo, P.G., 2000. Discrete sedimentation model for ideal suspensions. Chemical Engineering Journal 80, 135–140.

Richardson, J.F., Zaki, W.N., 1954. Sedimentation and fluidization: part I. Transactions of the Institution of Chemical Engineers 43, 35–53.

Selim, M.S., Kothari, A.C., Turian, R.M., 1983. Sedimentation of multisized particles in concentrated suspension. A.I.Ch.E. Journal 29 (6), 1029–1038.

Takacs, I., Patry, G., Nolasco, D., 1991. A dynamic model of the clarification-thickening process. Water Research 25, 1261271.

Vesilind, P.A., 1979. Treatment and Disposal of Wastewater Sludges. Ann Arbor Science, Ann Arbor, MI.

Watts, R.W., Svoronos, S.A., Koopman, B., 1996. One-dimensional modelling of secondary clarifiers using a concentration and feed velocity-dependent dispersion coefficient. Water Research 30 (9), 2112–2124.

Williams, R.A., Amarasinghe, W.P.K., 1989. Measurement and simulation of sedimentation behaviour of concentrated polydisperse suspensions. Transactions of the Institution of Mining and Metallurgy 98, C68–C82.

Zheng, Y., Bagley, D., 1998. Dynamic model for zone settling and compression in gravity thickeners. Journal of Environmental Engineering 124 (10), 95958.

Zimmels, Y., 1983. Theory of hindered sedimentation of polydisperse mixtures. A.I.Ch.E. Journal 29 (4), 669–675.

Zeidan, A.M., Rohani, S., Bassi, A., Whiting, P., 2003a. Review and comparison of solids settling velocity models. Reviews in Chemical Engineering 19 (5), 473–530.

Zeidan, A.M., Rohani, S., Bassi, A., Whiting, P., 2003b. Biosys: software for wastewater treatment simulation. Advances in Engineering Software 34 (9), 539–549.